united nations
educational, scientific
and cultural
organization

international atomic
energy agency

the
abdus salam
international centre for theoretical physics

SMR/1328/28

School on the Physics of Equatorial Atmosphere

(24 September - 5 October 2001)

Techniques for Airglow Measurements

R. Sridharan
(Vikram Sarabhai Space Center, Trivandrum)

Techniques for Airglow measurements:

The critical elements needed for the measurement of faint airglow emissions are ***(1) narrow band interference filter (2) a dispersing element*** in the case of a spectrometer ***and (3) a sensitive detector*** suitable for the wavelength band of interest.

Interference filters: Narrow band interference filters permit the isolation of the wavelength interval down to a fraction of a nanometer without the use of a dispersing element like a prism, grating or any other device. Coloured glass and gelatine filters cannot do the job.
They come in two kinds:

(1) Edge filter
(2) Band pass filters

Typically the transmission of a filter ranges anywhere between 35-50%. It is strongly dependent on the bandwidth. The narrower it is, lesser would be transmissivity.

Effect of angle of incidence: *Both the transmittance and reflectance shift to shorter wavelengths as they are tilted from normal to oblique incidence. For smaller angles the shift is without much distortion or reduction in peak transmission.*
The conditions for interference

$$2\mu t \cos\theta = n\lambda$$

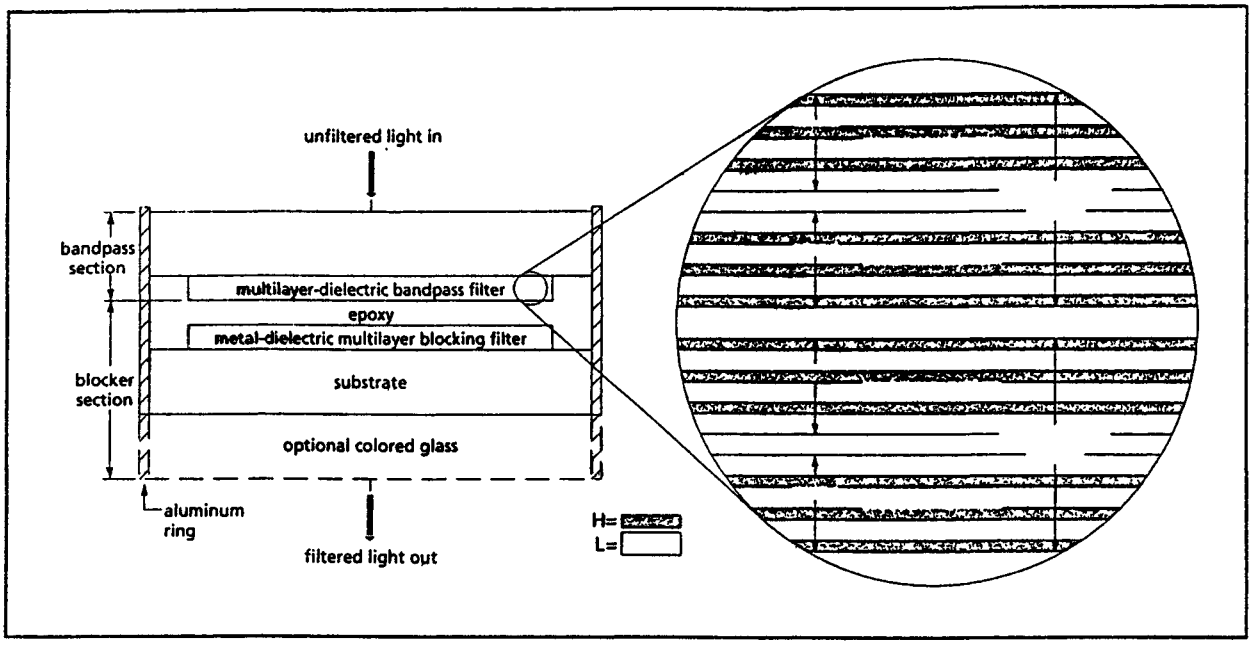

Cross section of a typical two-cavity pass interference filter

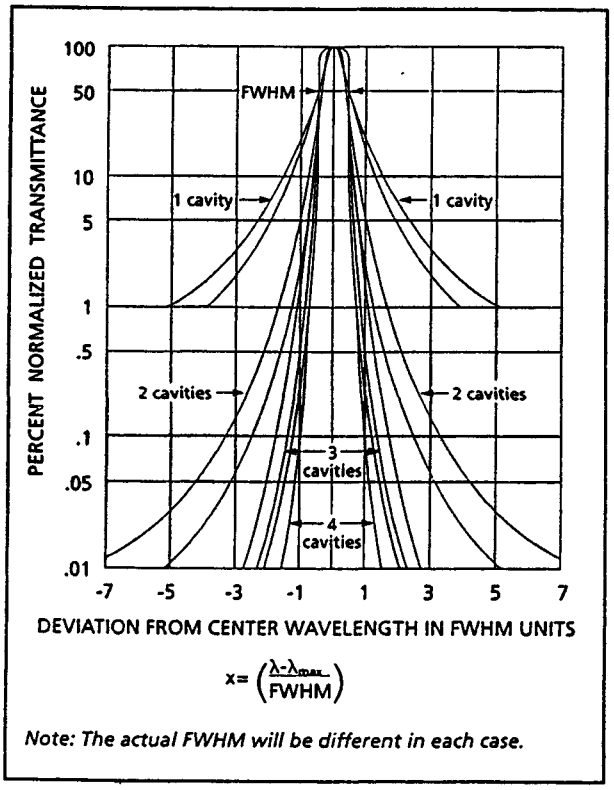

Normalized log scale transmittance curves for ZnS/Na_3AlF_6 bandpass interference filters of 10 nm FWHM as functions of the number of cavities used in filter construction

Filter characteristics :

Effect of incident angle θ

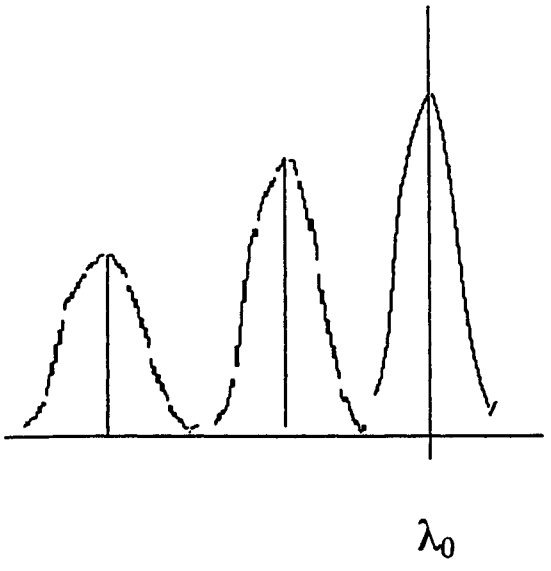

Effect of temperature

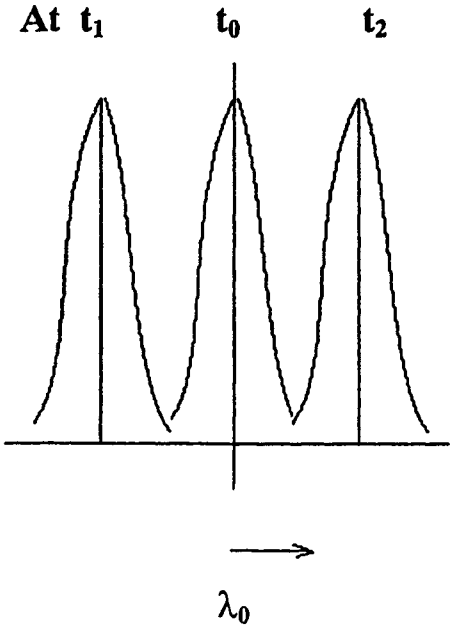

Where μ is the reflective index, t is the thickness of the film θ the angle of incidence and `n' the order of interference (a nonzero quantity) and λ is the wavelength of the resonant peak.

In the case of an interference filter the transmitted spectrum is ***temperature dependent.*** *With the increase of temperature the layer thickness increase. At the same time refractive index of allthe layers change. They combine in such a way that the peak transmission shifts to higher wavelength side. The thermal coefficient is a function of wavelength.*

Photomultipliers: Cover the same range as that of a photographic plate - Below 2000 A which is the transmission limit of quartz, two adaptations are possible.

(i) The most commonly used window of the conventional photo multiplier is coated with a phosphor (usually sodium salicilate) which converts the incident light to sufficiently long wavelength to get through the window. The efficiency of this process drops, once the incident wavelength goes below 1000 A and remains at the same level upto even 300 A.

(ii) Alternately open phtomultipliers which have dynodes or metal cathode which does not get poisoned by exposure to atmosphere have also been used in spectrograph in vacuum or in a separately pumped chamber.

However, the high work function of the cathode prevents detection of longer wavelength > 2000 A. These are sometimes called **`Solar blind'.**

Comparison between photographic plate and a photomultiplier

Photographic plate	Photoelectric detector
Long integration possible	**Superior in terms of time resolution**
Multiplex advantage – Simultaneous detection of many spectral elements	**Linear response and extremely useful in intensity measurements**
10^7 - dynamic range	**10^9 –dynamic range**
Best suited for transient phenomenon like flashes	**Best suited for continuous sources**
Spatial resolution of few μm	**Time resolution in nano sec.**
Measures energy/area	**Measures energy/time**

PMTs typically have gains of 10^6-10^7

The spectral response is decided by the 'Quantum efficiency' of the photo cathode material

The Dark currents are of the order of 10^{-15}A – 10^{-14}A.

Detectors: Human eye has a limited range of sensitivity i.e. 4000-7000A.

Till recently, the most widely used detector is the photographic plate ($\lambda\lambda$ = 2300 – 7000 A. Extendable up to 12000 A with poor sensitivity)

In the UV range plates without gelatine are sensitive up to x-rays but the contrast is rather low.

Photomultipliers are extremely sensitive devices providing a current output proportional to the incident intensity.

The PMT detects light at the photocathode (k) which emits electrons by the photoelectric effect. The photoelectrons are electrostatically accelerated and focussed on to the first dynode. On impact each electron liberates more than one secondary electron which in turn are accelerated and focussed on to the subsequent dynode. This process gets repeated and the multiplied secondary electrons are collected by the anode. By appropriately controlling the accelerating voltages and also the EHT, the PMT can be used over a wide dynamic range.

Photocathode material is chosen for the specific application (spectral response)

The Quantum Efficiency (%) = Average photoelectric yield/incident photon

Dark current and the time response of the PMT are crucial for any application.

Detectors for the Ultraviolet:

In addition to special photographic plates and PMT, detection by direct photoionisation also becomes possible below 1300 A (> 9 ev). Permanent gases could be ionised. Once operated in the plateau region of the I-V curve, the ion current becomes independent of the voltage and is directly related to the incident intensity. The efficiency could be 100% or more! The pulsed version is nothing but a Geiger counter. The initial photoelectron is accelerated and made to collide with the other molecules so that some sort of an avalanche effect takes place using gas amplifications.

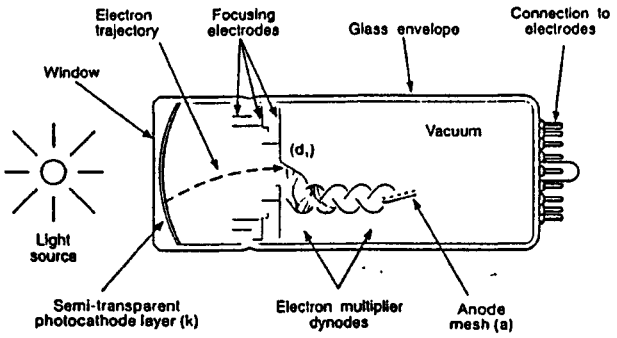

Figure 1

Illustrating the operation of a photomultiplier.

3 The Photocathode

This section gives information on:

- the light sensitive area of the photomultiplier
- the effect of the window on light transmision
- photocathode spectral response
- photocathode sensitivity units

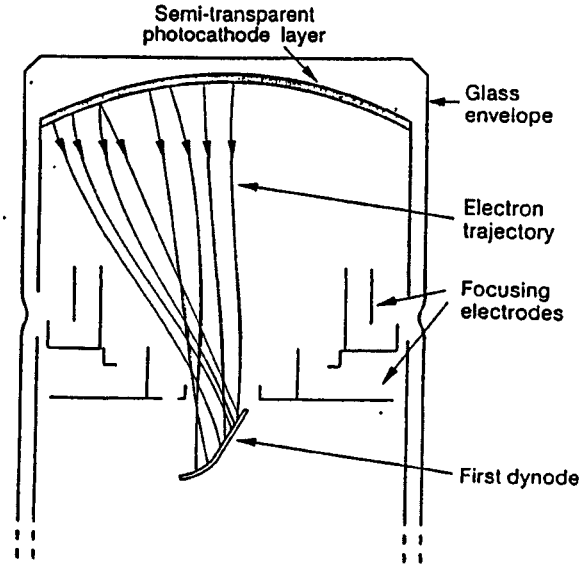

Figure 8

Photoelectron trajectories between photocathode and first dynode.

3.1 Photocathode Active Area

Photomultipliers are offered in a range of geometries and sizes to cover applications involving both remote and directly coupled light sources. In end window photomultipliers, the photocathode is deposited as a semitransparent layer directly on the inside of the window. In the majority of types the active area has a circular geometry (Figure 2a). Some have a reduced active area, achieved by electrostatic focusing, which can be an advantage in the detection of very weak light sources (Figure 2b). Special photocathode geometries,(Figures 2 c, d and e), have been introduced for large volume, extended area and large solid angle applications.

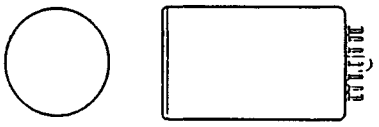

a) Circular

Range of diameters available to suit diffuse and directly coupled light sources.

Application: General purpose; scintillation.

b) Reduced

Electrostatically reduced diameter for minimum dark count.

Application: Photon counting and laser light detection.

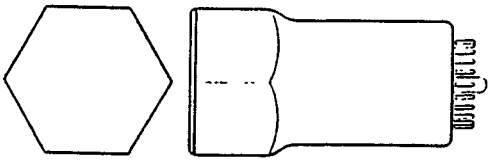

c) Hexagonal

Close packing allows maximum coverage of large areas.

Application: Gamma Camera.

d) 2π

Side wall sensitivity allows wide angle detection.

Application: Probes for radiation monitoring.

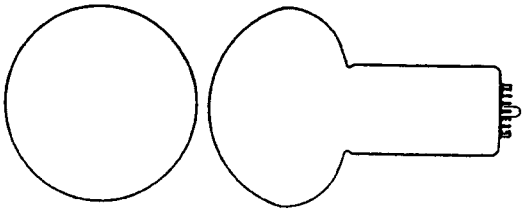

e) Hemispherical

For diffuse light sources, e.g. arrays of photomultipliers.

Application: Fundamental scientific research.

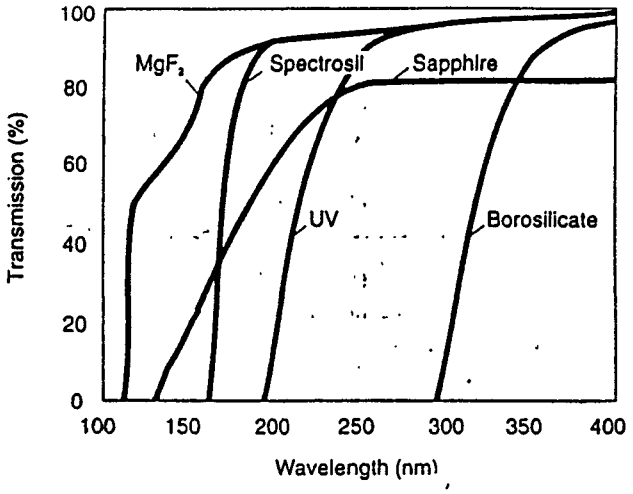

Figure

Typical UV transmission curves for windows used in the manufacture of THORN EMI photomultipliers.

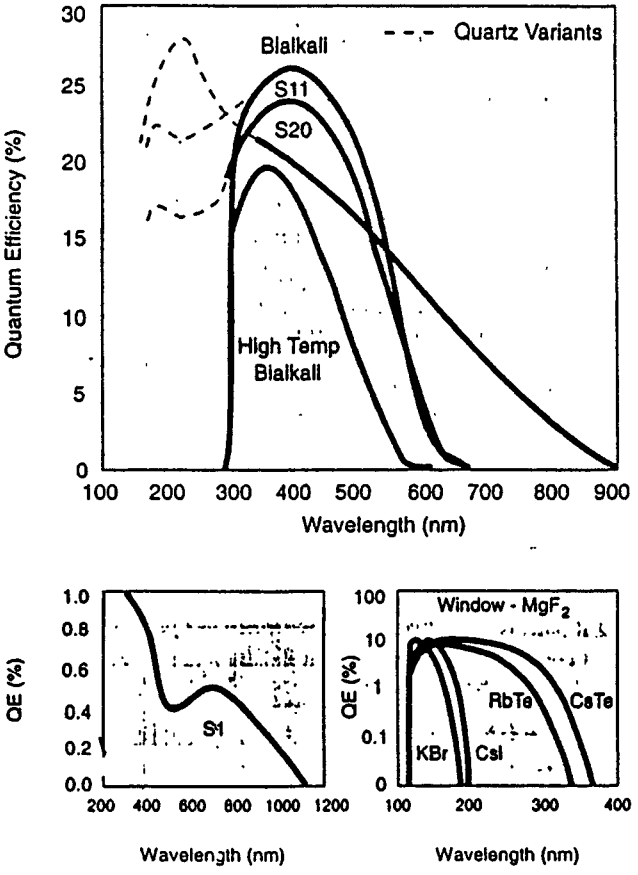

Figure

Typical spectral response curves for 52 mm diameter photomultipliers.

Both these types cannot be used in the λ λ 1040 - 300 A for want of a suitable window material. < 300 A cellulose and thin metal films start transmitting.

Detector for the Infra Red

Since at λλ 13000 A has insufficient energy to cause ionisation or activate an emulsion it is very difficult to detect this radiation.

IR detectors are of two types

(i) Thermal type
(ii) Photoconductive

In both the cases response is proportional to the power absorbed (W) and they measure the power absorbed in unit time, independent of the wavelength.

Photo conducting type measures the rate at which photons are absorbed.

$$\frac{dn}{dt} = \frac{W}{h\nu} \qquad (1)$$

Ideally their response increases with increase of λ for constant power over the sensitive range.

Response time

Thermal detectors	-	ms	⎫	
Photo conductive type	-	μs	⎬	noisy too
Photomultiplier	-	ns	⎭	

Photoconductive cells are semi conductors whose electrical resistance decreases when exposed to light. The change in resistance is proportional to the rate at which photons are absorbed and can be detected as a change in voltage across a load resistor in series with the photoconductor.

The photons do not have sufficient energy to release an electron out of the surface, but below a certain cut off level they have enough energy to free an electron from the crystal lattice and so increase the number of free electrons and/or holes that act as current carriers.
This effect is enhanced by cooling the semiconductor to reduce the number of thermally excited electrons. PbS, and InSb are some of the standard IR detectors and the technology is continuously being upgraded.

The ultimate useful sensitivity of the detector is limited by the noise. For detection S/N ratio > 1

Noise could be of three origins:

(1) Fluctuations in the background radiation and in the light source itself

(2) Electrical and thermal fluctuations in the detector

(3) Noise originating in the amplifier part.

Various techniques like chopping the detector improve the performance and following phase sensitive detection, cooling the detector to reduce the thermal noise are some of the standard methods to reduce the noise of detector origin.

Visible range	-	limited by photon noise
I_R thermal detector	-	thermal noise
I_R photo conductive	-	current noise

External factors

Temperature, Magnetic fields, Electric fields, Ionizing radiation and Exposure to daylight are external factors which increase the noise.

Interference Filter Usage

Narrowband interference filters are extremely angle sensitive. The transmittance of a 1.0-nm FWHM filter will fall by 10%, at the transmission wavelength, for field angles of only 2.5 degrees. For field angles of five degrees, the transmittance falls by over 90%. It is important, therefore, to use narrowband interference filters in locations that ensure maximum collimation. The illustration shows the design of a narrow-field spectral radiometer for infinite conjugate ratio use, and it indicates the proper interference filter location. The radiometer consists of an interference filter, objective lens, field lens, field stop, and detector. The field lens, which images the objective lens onto the detector's sensitive area, ensures uniform illumination of the detector. The field of view is limited by a field stop placed close to the field lens.

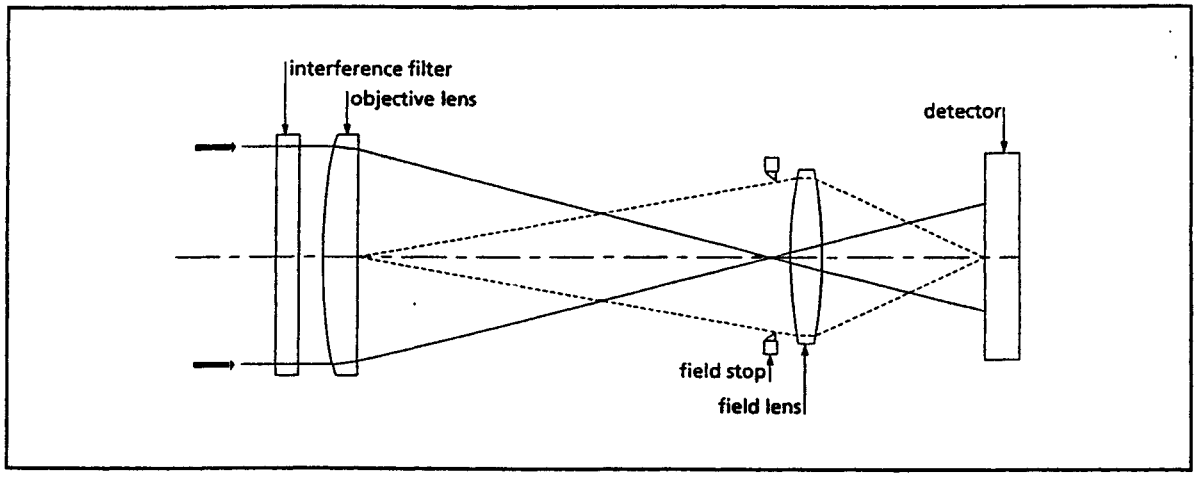

Line Profiles

In general it is presumed that the spectral lines do not have any spread in frequency/wavelength scale and all the spread that is observed when measurements are made is usually ascribed to the instrument - referred to as ***the instrumental width.***

In reality there can never be an ideal monochromatic line, as they would always have a finite width.

The different processes that contribute to the line width are,

(i) Natural broadening
(ii) Doppler broadening and
(iii) Pressure broadening

Natural broadening: Absorption or emission of a photon consists of transitions from one discrete energy level to another. These levels cannot be infinitely narrow because the uncertainty principle in the form of

$$\Delta E \,.\, \Delta t = \hbar \tag{2}$$

requires the energy spread to be

$$\Delta E = \hbar / \Delta t \tag{3}$$

Where `Δt' is the uncertainty in time associated with finding the atom in that particular state and is measured by the mean life time `τ' of the state.

The frequency spread for the state `j' can then be written as

$$\delta \nu_j = \frac{1}{2\pi \tau_j}$$

δ_{vj} is negligible for the ground state or a meta-stable state ($\tau_j \rightarrow \infty$) . The upper state of allowed transitions have lifetime of the order of
10^{-6} - 10^{-9}s. Any spectral line starting or finishing at this energy level must then have a corresponding spread E in frequency which is of the order of 0.1 to 100 MHz.
The width of the line is given as

$$\delta \nu_{12} = \delta \nu_1 + \delta \nu_2$$

Natural broadening decreases rapidly in the infrared and μ wave regions It may become appreciable in the far UV. In the visible
it is normally two orders of magnitude smaller than the Doppler broadening.

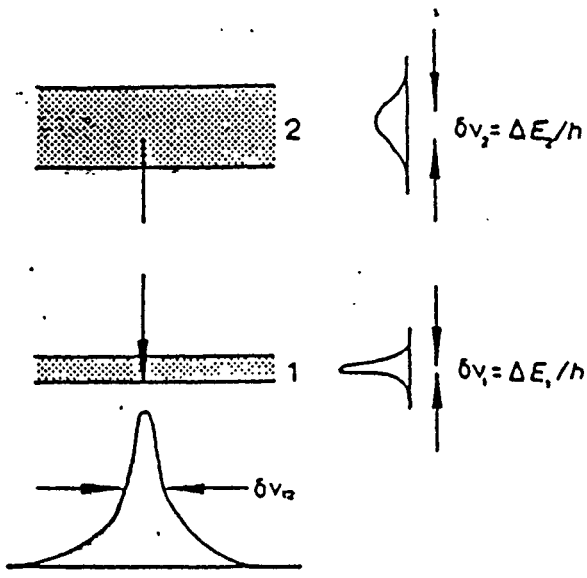

Fig. . Natural broadening of spectral line. The energy levels are smeared out according to the probability distribution shown on the right of the diagram. The half-value width of the spectral line is $\delta\nu_{12} = \delta\nu_1 + \delta\nu_2$ (see text).

Doppler Broadening:

Doppler broadening of any spectral line is a result of the well known `Doppler effect' which is the apparent shift in wavelength of the signal from a source moving towards or away from the observer. When the motion is towards the observer, it could cause a decrease in wavelength or increase in frequency. When it is away, the reverse happens i.e., there would be an increase in wavelength and decrease in frequency.

The Doppler effect in sound waves is experienced in every day life. The famous red shift of the expanding universe in cosmology is also well known.

Even when the light source is stationary the light emitting or absorbing atoms or molecules are moving and it is logical to expect that any component of velocity directed away or towards an observer will give rise to a red or blue shift respectively. A large number of atoms having different velocities will emit a broadened line i.e., a spread in wavelength. Specifically for an emitter approaching the observer with velocity `u' the Doppler shift in a line of wavelength λ_0 is given by

$$\lambda = \lambda_0 (1 + u/c) \tag{4}$$

$$\lambda - \lambda_0 = \lambda_0 (u/c) \tag{5}$$

$$u/c = \frac{\lambda - \lambda_0}{\lambda_0} = \frac{\Delta\lambda}{\lambda_0} \tag{6}$$

$$\frac{\Delta\lambda}{\lambda_0} = \frac{\Delta\nu}{\nu_0} = \frac{u}{c} \qquad (7)$$

If we know the proportion of atoms with a given velocity we can calculate the contribution to the spectral line at the corresponding wavelength and hence build up the line profile. If the motion is thermal - i.e., the gas is in thermal equilibrium at a temperature T - we do know this proportion. It is given by the Maxwell distribution.

$$dn_u = n/(\alpha\sqrt{\pi})\, e^{-u^2/\alpha^2}\, du \qquad (8)$$

Where dn_ν/n is the fraction of atoms having velocity between u and u+du along one axis (the line of sight in this case) and `α' is the (most probable velocity given by

$$\alpha = \sqrt{\frac{2kT}{m}} = \sqrt{\frac{2RT}{M}} \qquad (9)$$

Where `m' is the mass and `M' is the mass number.

`k' is the Boltzman's constant and `R' the universal gas constant.

Substituting for `u' from (7) into (8) one can obtain the fraction of atoms emitting in the frequency interval `ν' and `ν + d ν'

$$\frac{dn_\nu}{n} = \frac{1}{\alpha\sqrt{\pi}}\, e^{-c^2(\Delta\nu)^2/\nu^2\alpha^2}\, \frac{C}{\nu_0}\, d\nu \qquad (10)$$

Since the intensity at `ν' is proportional to dn_ν, the line profile can be written in terms of central frequency I_0 as

$$I_\nu = I_0 \, e^{-c^2(\nu_0 - \nu)^2 / \nu^2_0 \alpha^2} \tag{11}$$

This is Gaussian distribution about the central frequency ν_0 with a width determined by `α'.

$$I_\nu = \frac{1}{2} I_0 \tag{12}$$

The half intensity points are the values of $\nu_{1/2}$ for which

$$\frac{c^2}{\nu_0^2 \alpha^2} (\nu_0 - \nu_{1/2})^2 = \ln 2 \tag{13}$$

The half value width `$\delta\nu_D$' is therefore, $\delta \nu_D = |\nu_0 - \nu_{1/2}| \times 2$

$$\delta\nu_D = \frac{2\nu_0}{c}\sqrt{\frac{2RT}{M}} \ln 2 \quad \text{Substituting for `}\alpha\text{'} \tag{14}$$

$$\boxed{\delta\nu_D = 7.16 \times 10^{-7} \nu_0 \sqrt{\frac{T}{M}}} \tag{15}$$

This can be expressed in a dimensionless form

$$\frac{\delta\nu_D}{\nu_0} = \frac{\delta\lambda_D}{\lambda_D} = \frac{\delta\sigma_D}{\sigma_D} = 7.16 \times 10^{-7} \sqrt{\frac{T}{M}} \qquad (16)$$

The Doppler distribution is often written in terms of the half value width as

$$I = I_0 \exp(-y^2) \qquad (17)$$

with

$$y = \frac{2(\nu_0 - \nu)}{\delta\nu_D} \sqrt{\ln 2} \qquad (18)$$

Pressure broadening:

It is a well known experimental fact that as the pressure in an emitting or absorbing gas is increased the spectral lines are broadened and in many cases are shifted. Sometimes additional lines (due to forbidden transitions) may also appear.

These are essentially due to the interaction with other particles.

In the ionosphere/thermosphere regions, the pressure broadening effects are literally non-existent.

Interferometers:

For very high resolution spectroscopy only two types of instruments are important.

(1) The Fabry Perot Spectrometer (FPS) and

(2) The Michelsons Interferometer (MI)

The FPS is a multiple beam instrument capable of very high resolution and usable in the near Infrared to Quartz UV.

The MI, on the other hand, is a two-beam interferometer whose present importance comes from its use as a scanning instrument to give a Fourier Transform of a spectrum. Ideally suited for the infrared range.

Fabry- Perot Interferometer:

The FP consists of two glass plates (fused silica) separated by a distance `t', held accurately parallel to each other.

The plates are finely polished to better than $\lambda/100$ and the spacers are optically bonded to the plates.

An FPI set up with such a spacer is known as an `etalon'.

The facing surface of the plates are coated with very highly reflecting dielectric coating (typically ~90% reflectivity).

A light ray incident t at an angle `$\theta$', undergoes multiple reflections. Successively reflected rays emerge parallel with a constant path differences `Δ'.

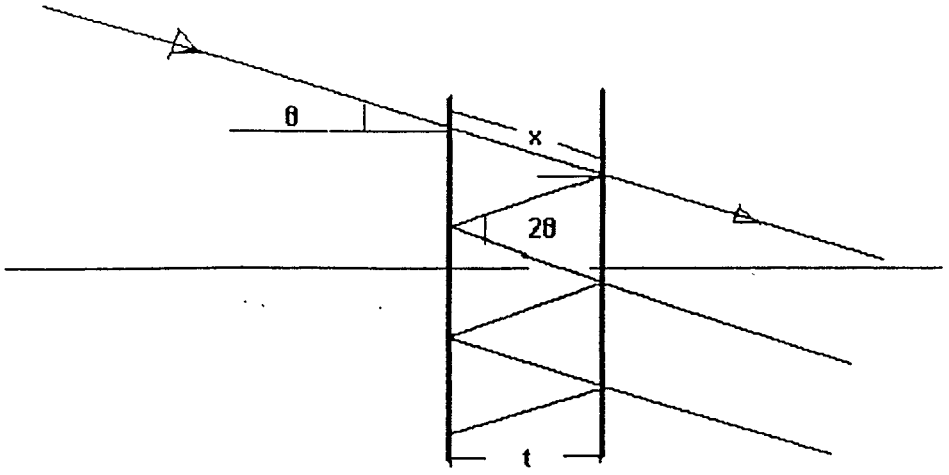

path of a light ray through a Fabry-Perot inerferometer

t/x = cos θ

x= t/cos θ

The path difference PD is given by

$$\Delta = x(1+Cos\ 2\theta)\ where \quad x = t/Cos\ \theta \tag{19}$$

$$\Delta = \frac{t}{Cos\ \theta}(1+Cos\ 2\theta) = \frac{2t\ Cos^2\theta}{Cos\theta} = 2t\ Cos\ \theta \tag{20}$$

Taking the refractive index `μ' into account

$$\Delta = 2\mu t\ Cos\ \theta \tag{21}$$

If `Δ' is an integral multiple of `λ', the incident wavelength interferes constructively and hence maximum intensity would occur i.e.,

When $2\mu t\ Cos\ \theta = n\lambda$, maximum intensity occurs.

The FP fringes are made up of equal inclination rays: The interference fringes have cylindrical symmetry about the optical axis, and therefore the interference pattern produced by the monochromatic light is a set of concentric rings. With the radii of intensity maxima being given as (fθ) - f being the focal length and `θ' the angle of incidence.

Cos θ decreases with the increase of `θ, and hence the order of interference is highest at the centre.

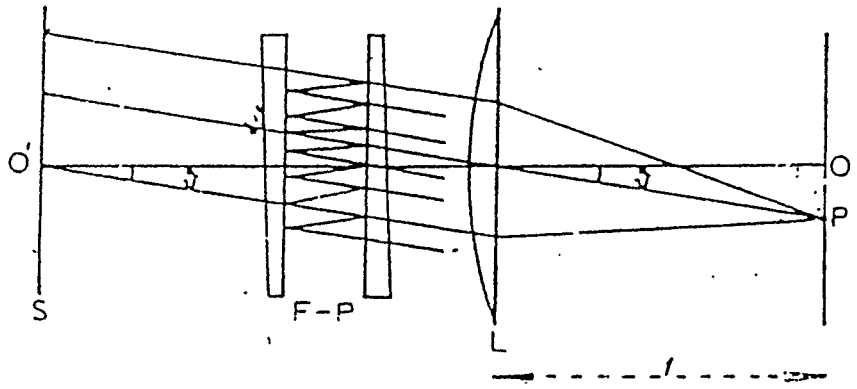

Fig. . Optical arrangement for Fabry–Perot interferometer. The figure shows the paths of those rays from all points of the source that are inclined at angle θ to the axis. Only a few of the multiple reflections are shown. The wedge angles of the Fabry–Perot plates (see text) are much exaggerated.

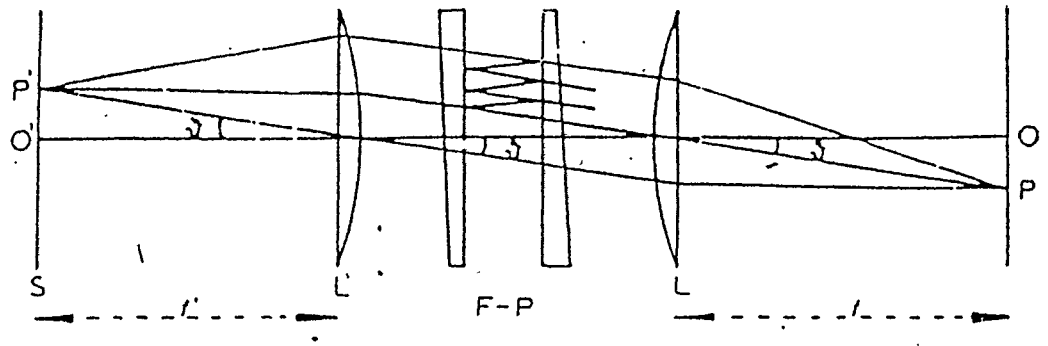

Fig. . Optical arrangement with source imaged in same plane as fringes. Lens L′ has been added to Fig. 6.2. The only rays incident on the interferometer at angle θ now *all* come from the point P′.

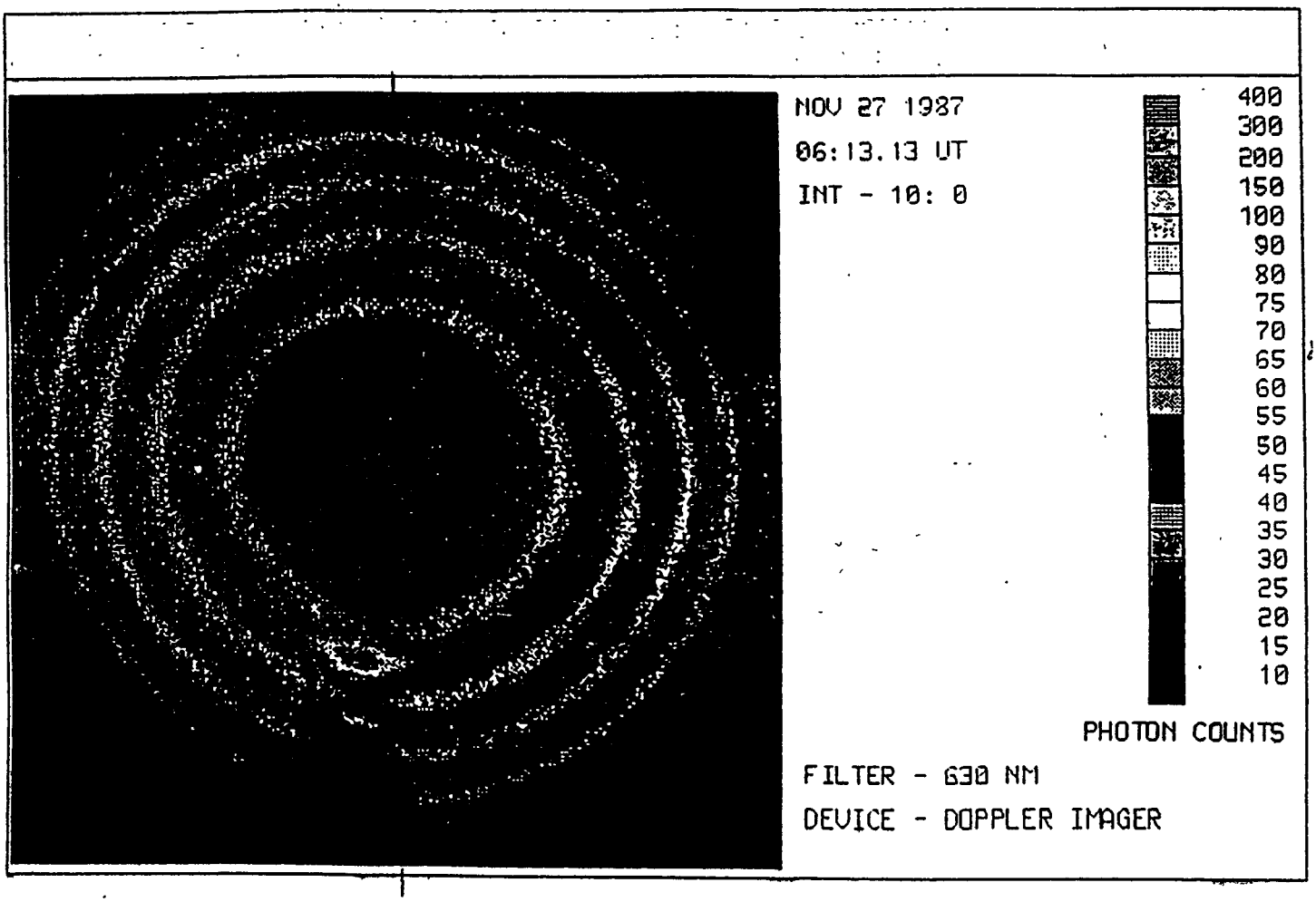

Figure : A full two-dimensional image of the sky obtained by the DIS under conditions of moderately active auroral activity at 06.13 UT on 27th November 1987. North is at the top, east to the right.

Dispersion and free spectral range

Let us start with

$$2\mu t \cos\theta = n\lambda \qquad (22)$$

Angular dispersion

$$\frac{d\lambda}{d\theta} = \frac{1}{n} 2\mu t \sin\theta \qquad (23)$$

For $\mu = 1$ and for small angles $\sin\theta = \theta$

From equation 22 $2t = n\lambda$; $n = \frac{2t}{\lambda}$

Substituting in 23

$$\frac{d\lambda}{d\theta} = \frac{\lambda}{2t} 2t\theta = \lambda\theta \qquad (24)$$

or

$\frac{d\theta}{d\lambda} = \frac{1}{\lambda\theta}$ - *The angular dispersion is independent of 't'*

To illustrate order of magnitude

The reciprocal linear dispersion at 1 mm from the centre for λ = 500 A

With `f' in cm. $\theta = 0.1/f$

Linear dispersion

$$\frac{d\lambda}{d\ell} = \frac{d\lambda}{d(f\theta)} = \frac{1}{f}\ \frac{d\lambda}{d\theta} = \frac{1}{f}\lambda\theta. = \frac{\lambda(0.1)}{f.f}$$

ie.

$$\frac{d\lambda}{d\ell} = \frac{0.1\lambda}{f^2}$$ for f = 50 cm it is 0.02 A/mm

Which is an order of magnitude better than any grating instrument except large echelle grating which is a far bulkier instrument.

However, the order number in a FP is from one to three orders of magnitude higher than in an echelle and the problem of overlapping orders is correspondingly more severe.

For t = 1.0 cm and λ = 5000 A, $n = \frac{2t}{\lambda} = 4 \times 10^4$

Incidentally this order would coincide with the

40,001st order of 4999.88 A.

Which implies the free spectral range (FSR = $\lambda^2/2t$) is only 0.12 A.

It is sometimes convenient to work in wave numbers

$n\lambda = 2\mu t \cos\theta$ ie. $n = 2/\lambda\ \mu t \cos\theta = 2\sigma\ \mu t \cos\theta$

For $\mu = 1$ $\qquad$ **$n = 2\sigma t \cos\theta$** $\qquad$ **(25)**

For normal incidence $n = 2\sigma t$

Then

$$\therefore \quad \Delta n = 2\Delta\sigma t \quad \textbf{when } \Delta n = 1 \textbf{ ie the FSR} \qquad (26)$$

$\Delta\sigma = \frac{1}{2t}$ **for t = 1.0 cm the range between orders is 0.5 cm^{-1}**

I

intensity distribution in the interference pattern:

As one cuts across the interference pattern of a FP etalon, maxima and minima are encountered.

Maximum occurs when $n\lambda = 2\mu t \cos\theta = 2t\cos\theta$

and minimum when $(n + \frac{1}{2})\lambda = 2t\cos\theta$

If `s' and `r' are the fractions of transmitted and the reflected rays (s is used to avoid mix up with `t' the spacing between the reflecting surface)

The amplitude of the incident ray is A_0 and the transmitted ray is $A_0 S^2$. If the phase difference between successive rays is denoted by δ

$$\delta = 2\pi\frac{\Delta}{\lambda} = \frac{4\pi t\cos\theta}{\lambda} = 4\pi\sigma t \cos\theta \qquad (27)$$

When all these rays are superposed in the focal plane of a lens, the resultant amplitude is

$$A = \left(A_0 s^2 \left(1 + r^2 e^{i\delta} + r^4 e^{2i\delta} + r^6 e^{3i\delta} + \ldots\ldots\ldots\ldots\right)\right) \qquad (28)$$

Which for a large number of rays turns out to be the sum of a geometric series

$$A = \frac{A_0 S^2}{(1 - r^2 e^{i\delta})} \qquad (29)$$

To get the intensity from the complex amplitude, A must be multipled by its complex conjugate

$$I = AA^* = \frac{S^4}{(1 - r^2 e^{i\delta})(1 - r^2 e^{-i\delta})} A_0 A^*_0 \qquad (30)$$

Introducing transmissivisity $T = s^2$, reflectivity $R = r^2$ and the intensity $I = AA^*$

$$I = \frac{T^2}{(1 - Re^{i\delta})(1 - R^2 e^{-i\delta})} I_0 = \frac{T^2}{(1 - 2R\,Cos\,\delta + R^2)} I_0 \qquad (31)$$

$$= \frac{T^2}{(1-R)^2 + 2R\,(1 - Cos\,\delta)} I_0 = \frac{T^2}{(1-R)^2 + 4R\,Sin^2\,\delta/2)} I_0 \qquad (32)$$

$$\therefore \quad I = I_0 \left(\frac{T}{1-R}\right)^2 \frac{1}{1+(4R/(1-R)^2)\mathrm{Sin}^2 \ \delta/2} \tag{33}$$

Is known as an `Airy distribution'

The maxima occur when

$\delta/2 = n\pi$ or $2\sigma t \mathrm{Cos}\,\theta = n$

From the Airy function

$$I_{max} = I_0 \left(\frac{T}{1-R}\right)^2 \tag{34}$$

In the ideal case of no absorption T + R = 1 and the peaks are transmitted without any loss.

The minima occur when δ is half way between the maxima.

i.e. when $\delta/2 = (n+1/2)\,\pi$ and would have an intensity

$$I_{min} = I_0 \left(\frac{T}{1+R}\right)^2 \tag{35}$$

The contrast of the fringes $\frac{I_{max}}{I_{min}}$ is given by

$$C = \left(\frac{1+R}{1-R}\right)^2 \text{ for R = 90\% ; C is a few hundreds} \quad (36)$$

The sharpness of the fringe critically depends on `R'.

The intensity distribution could also be written in wave number σ for fixed path difference Δ. Maxima occur for values of σ given by

$$\sigma = \frac{n}{\Delta} = \frac{n}{2t} = n\Delta\sigma \quad (37)$$

Where `$\Delta\sigma$' is the free spectral range (FSR)

The Airy distribution in terms of I_{max} as

$$I = \frac{I_{max}}{1 + f \sin^2 \delta/2}$$

or in terms of $\Delta\sigma$,

$$I(\sigma) = \frac{I_{max}}{1 + f \sin^2 / \pi\sigma/(\Delta\sigma)}$$

where $f = \frac{4R}{(1-R)^2}$

The finite spread of the fringes formed from a monochromatic light, measures the instrument function of the Fabry Perot.

In the absence of any other spreading function the half value width `$\delta\sigma$' can be written as:

Moving out by ½ δσ, the intensity will become I/2.

If

$$1+f\sin^2\left(\pi\frac{\delta\sigma}{2(\Delta\sigma)}\right)=2 \qquad (38)$$

i.e.,

$$\sin^2\left(\pi\frac{\delta\sigma}{2(\Delta\sigma)}\right)=\frac{1}{f}$$

For sharp fringes $\delta\sigma << \Delta\sigma$ and the sine term can be replaced by the angle to give

$$Sin\left(\frac{\pi\,\delta\sigma}{2(\Delta\sigma)}\right)=\frac{\pi\,\delta\sigma}{2(\Delta\sigma)}=\frac{1}{\sqrt{f}}. \qquad (39)$$

Substituting for f.

$$\therefore \quad \delta\sigma=\frac{2}{\pi\sqrt{f}}\Delta\sigma = \frac{1-R}{\pi\sqrt{R}}\,\Delta\sigma\,\frac{4R}{(1-R)^2} \qquad (40)$$

The Ratio of free spectral Range `Δσ' to that of the half width δσ measures the fine-ness or fine-sse. of the fringes and the coefficient `F' is defined by

$$F = \frac{\Delta\sigma}{\delta\sigma}=\frac{\pi\sqrt{f}}{2}=\frac{\pi\sqrt{R}}{1-R} \qquad (41)$$

Two lines cannot be resolved if the wave numbers do not differ at least by `δσ'. The resolving power is proportional to the finesse. F.

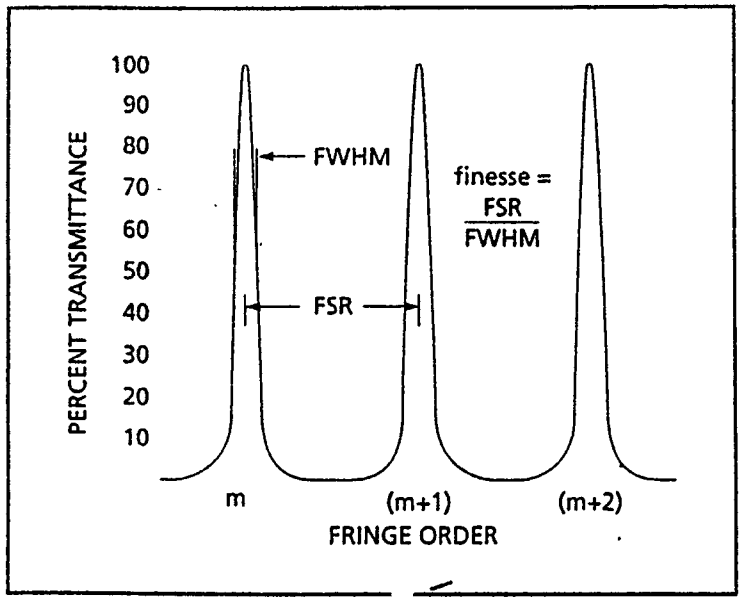

Transmission pattern showing the free spectral range (FSR) of a simple Fabry-Perot interferometer.

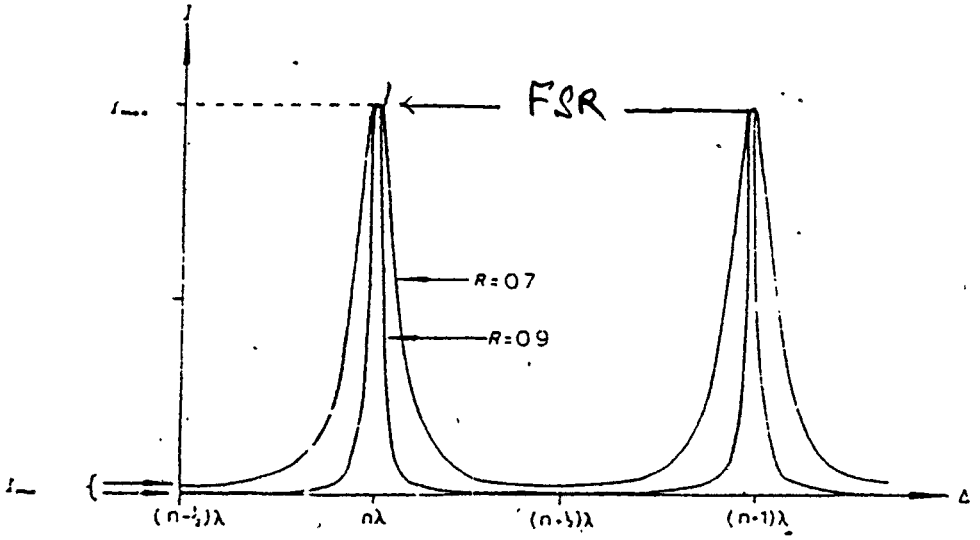

Fig. 6.5 Airy distribution as a function of path difference. The intensity distribution is shown for two different reflectivities, $R = 0{\cdot}7$ and $R = 0{\cdot}9$.

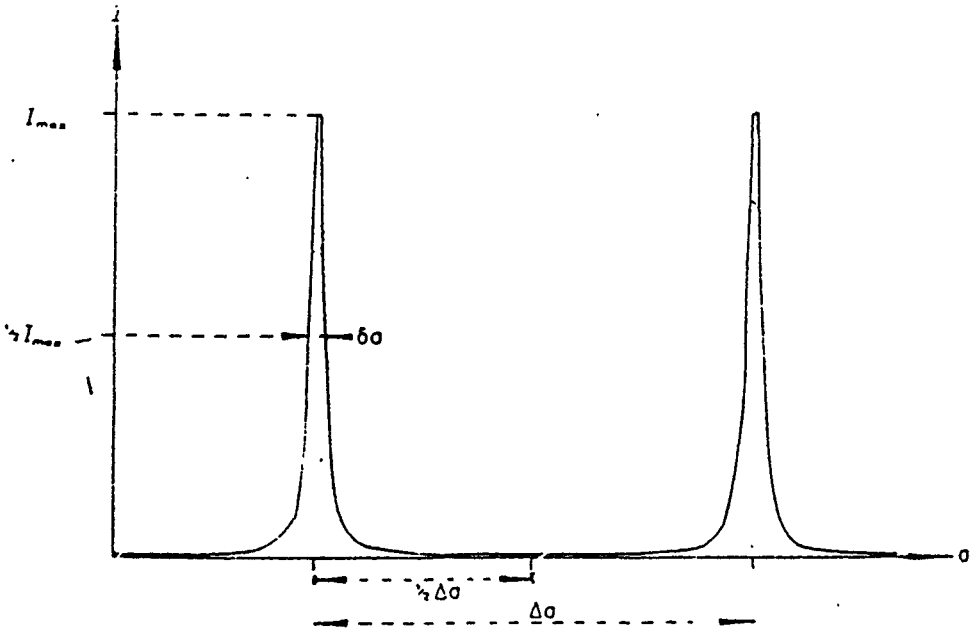

Fig. 6.6 Airy distribution as a function of wave number. $\Delta\sigma$ is the free spectral range. The intensity distribution is shown for $R = 0{\cdot}9$, and the half-value width $\delta\sigma$ in this case is 1/28 order.

Finesse increases with `R' the reflectivity

R	0.7	0.75	0.8	0.85	0.90	0.95
F	8.3	10.3	13.3	18.3	28.3	58

The above discussion is for an ideal case where there is no absorption

Realistically, accounting for absorption too,

$T=1-R-\Delta$

$$I_{max} = I_0 \left(1 - \frac{A}{I-R}\right)^2$$

Dielectric coatings enable very high reflectivity and very less absorption. Similar to an interference filter, high refractive (H) and low refractive ® index materials are coated alternatively with thickness of $\lambda/4$, beginning and ending with the H type of materials. The reflected rays will all be in phase for λ, and the reflectivity is maximum. As the number of layer is increased the reflectivity for `λ' increases while for other wavelengths it decreases.

In the visible region	98% reflectivity has been achieved
For UV (2500 A)	upto 90%
$\lambda < 2500$	80% achievable

Plate defects: *Irregularities in the plates even in the scale sizes of λ/150 could cause the reflected beams to be out of phase by 1/25 of an order. The fringe maximum therefore wanders by this much effectively reducing the 'finesse'. Ideally speaking both the reflective and the plate defect finesse should be made comparable.*

Resolving Power: *For an ideal etalon without any plate defects the half value width*

$$\delta\sigma = \frac{1-R}{\pi\sqrt{R}}\Delta\sigma = \frac{1}{F}\Delta\sigma \qquad (42)$$

Where 'F' is the finesse

At first it may appear that two superposed lines of equal intensities and separated by δσ would show no dip at all at the midpoint where each has half intensity to ½ Imax. However each line peak is lifted by the wings of the adjacent line to a value I_P.

Where

$$I_p = I_{max} + I_W \qquad (43)$$

I_W is the intensity at a wave number interval δσ from the maximum and can be found from the Airy function.

$$I_w = \frac{I_{max}}{1+f\sin^2\pi(\delta\sigma/\Delta\sigma)} \qquad (44)$$

For small angles sine could be replaced by the angle itself.

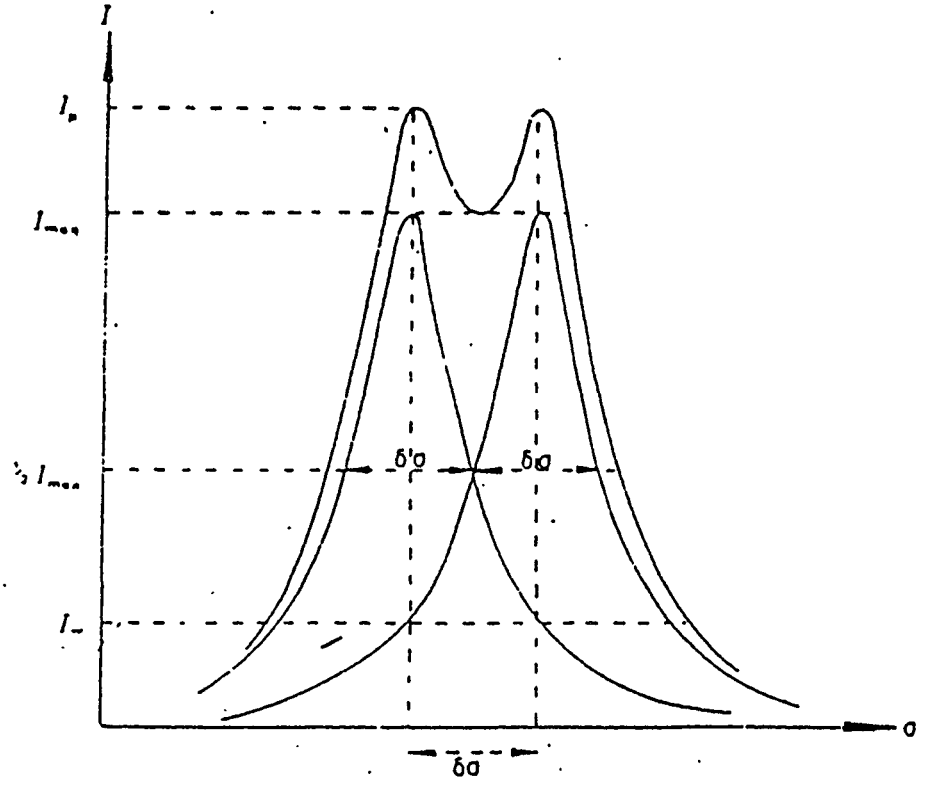

Fig. .. Rayleigh's .criterion applied to Fabry-Perot fringes. The peak intensity I_p is the sum of the maximum from one line, I_{max}, and the intensity I_w in the wing of the other line at $\delta\sigma$ from its centre.

$$\text{i.e.,} \qquad \sin^2 \pi \left(\frac{\delta\sigma}{\Delta\sigma}\right) = \pi^2 \left(\frac{\delta\sigma}{\Delta\sigma}\right)^2 = \frac{4}{f}$$

$$\textit{Since } I_w = \frac{I_{max}}{1+4} \textit{ and } I_p = \frac{6}{5} I_{max}$$

Θ The intensity at the dip is 83% of the peak; close to the requirement of the Rayleigh criterion. Consequently $\delta\sigma = \Delta\sigma / F$ holds for resolution as well as half value width. It is independent of the wave number and depends only on the reflectivity.

The resolving power therefore is

$$R = \frac{\sigma}{\Delta\sigma} = \frac{\sigma}{\delta\sigma} F = nF \quad \text{using} \quad n = 2t\sigma = \frac{\sigma}{\Delta\sigma}$$

For a finesse of 25; λ = 5000A; t = 1 cm.

$$R = 10^7 !$$

In practice 10^6 resolving power itself is quite useful. The plate defects would bring the theoretical resolution down by an order of magnitude and so are the other factors like the parallelism, and the finite aperture width.

HIGH RESOLUTION FABRY-PEROT SPECTROMETER (SCHEMATIC)

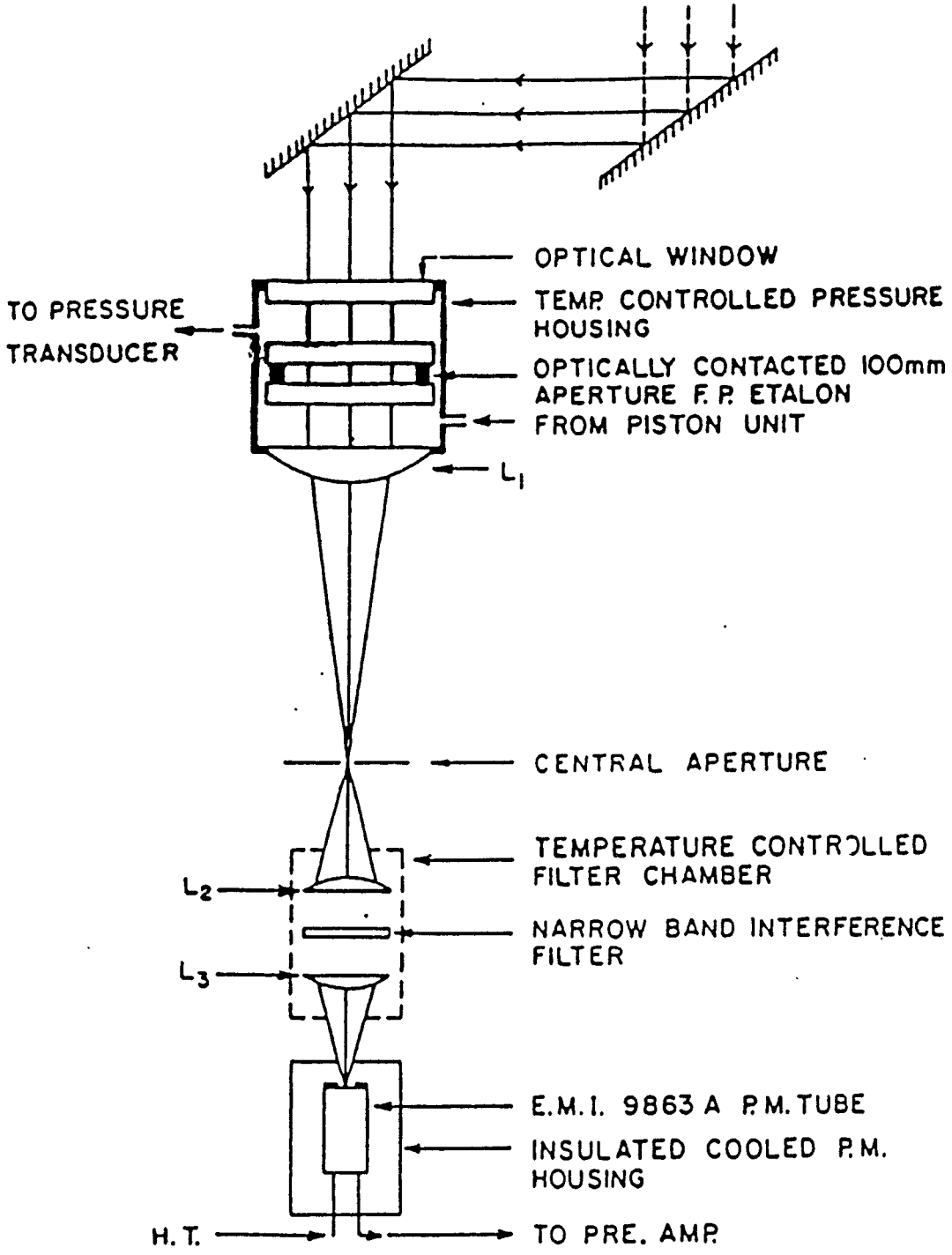

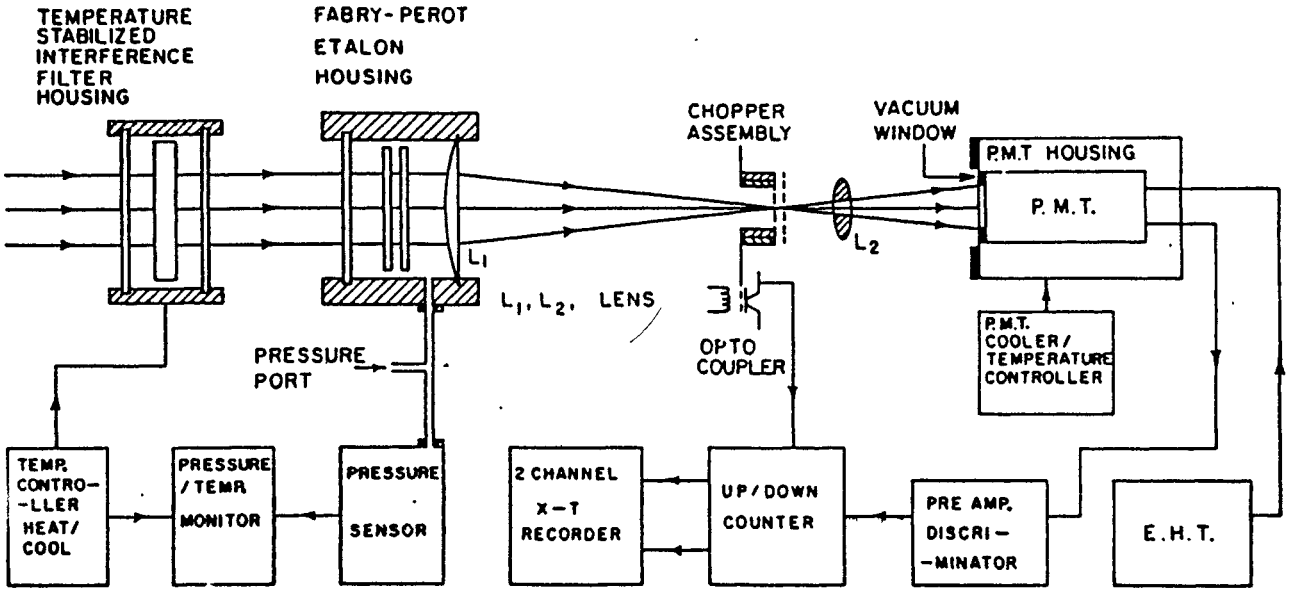

Fig. 1. Schematic diagram of the new dayglow photometer including the various electronic blocks.

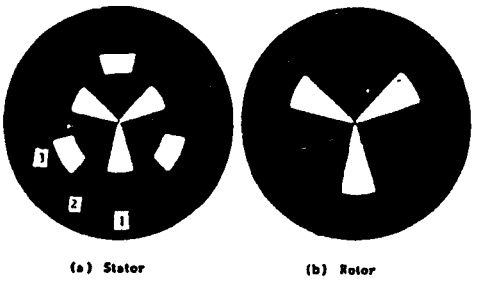

Fig. 2. New improved mask system that eliminates the problem of overlap between the inner and outer zones.

MULTI-WAVELENGTH DAYTIME PHOTOMETER

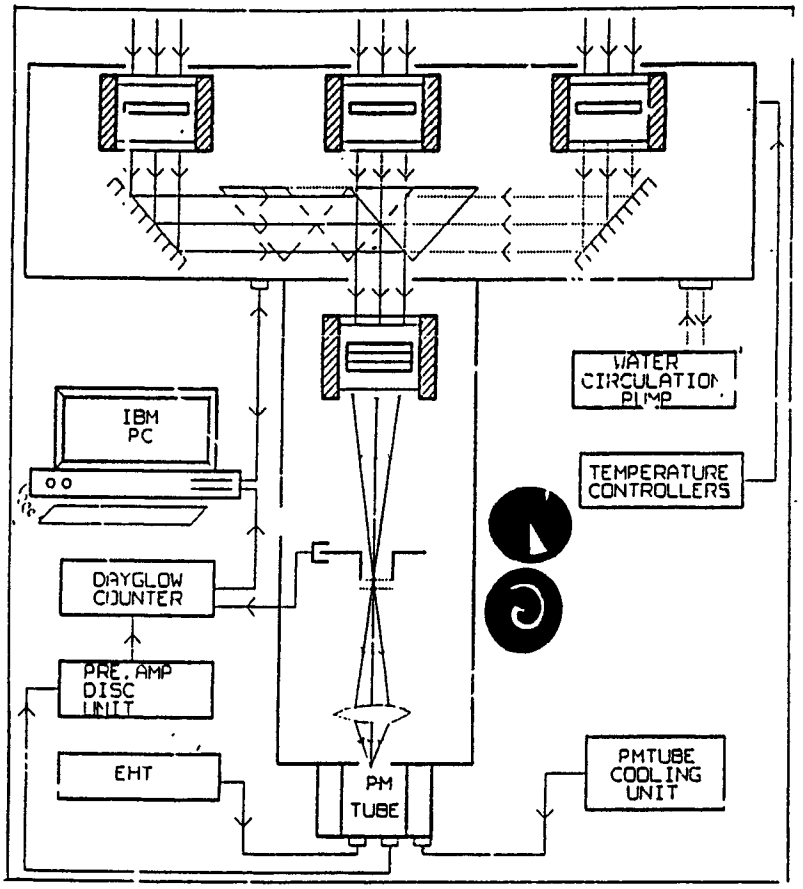

FIGURE 1

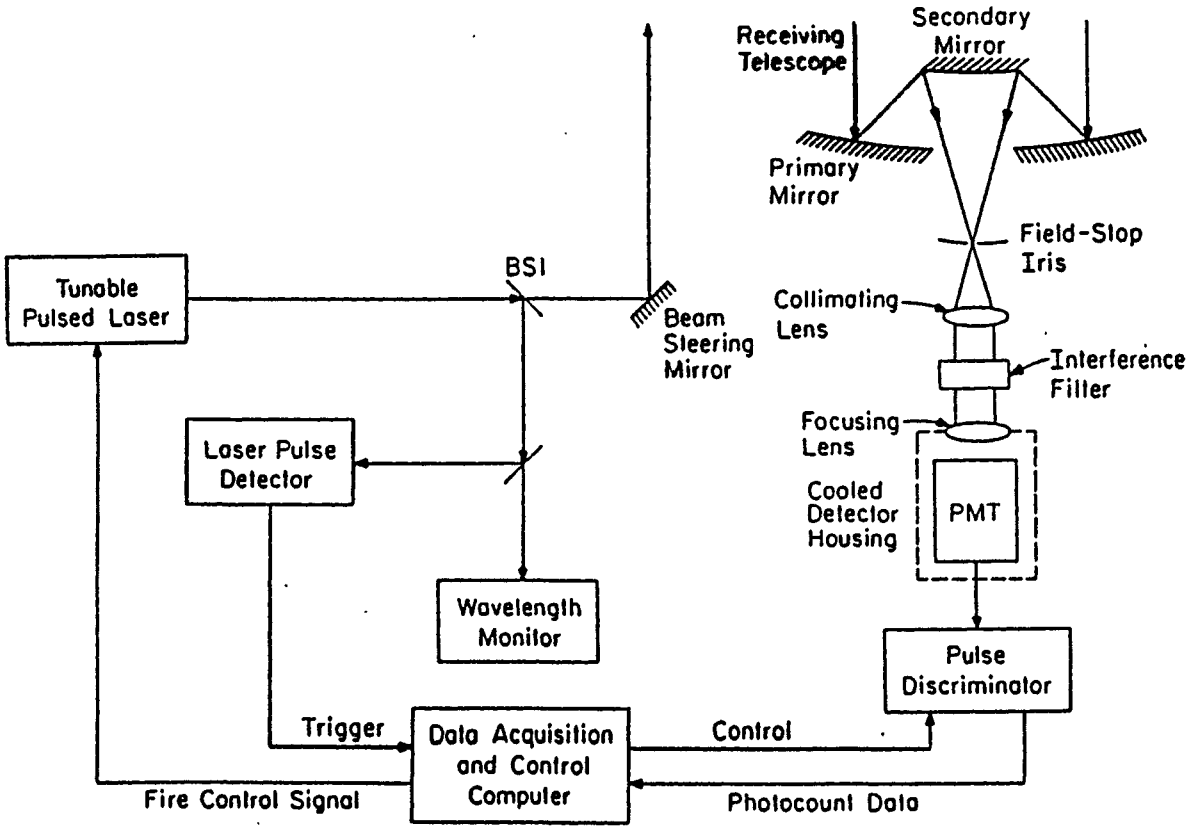

Figure Block diagram of a typical Na resonance fluorescence lidar system.

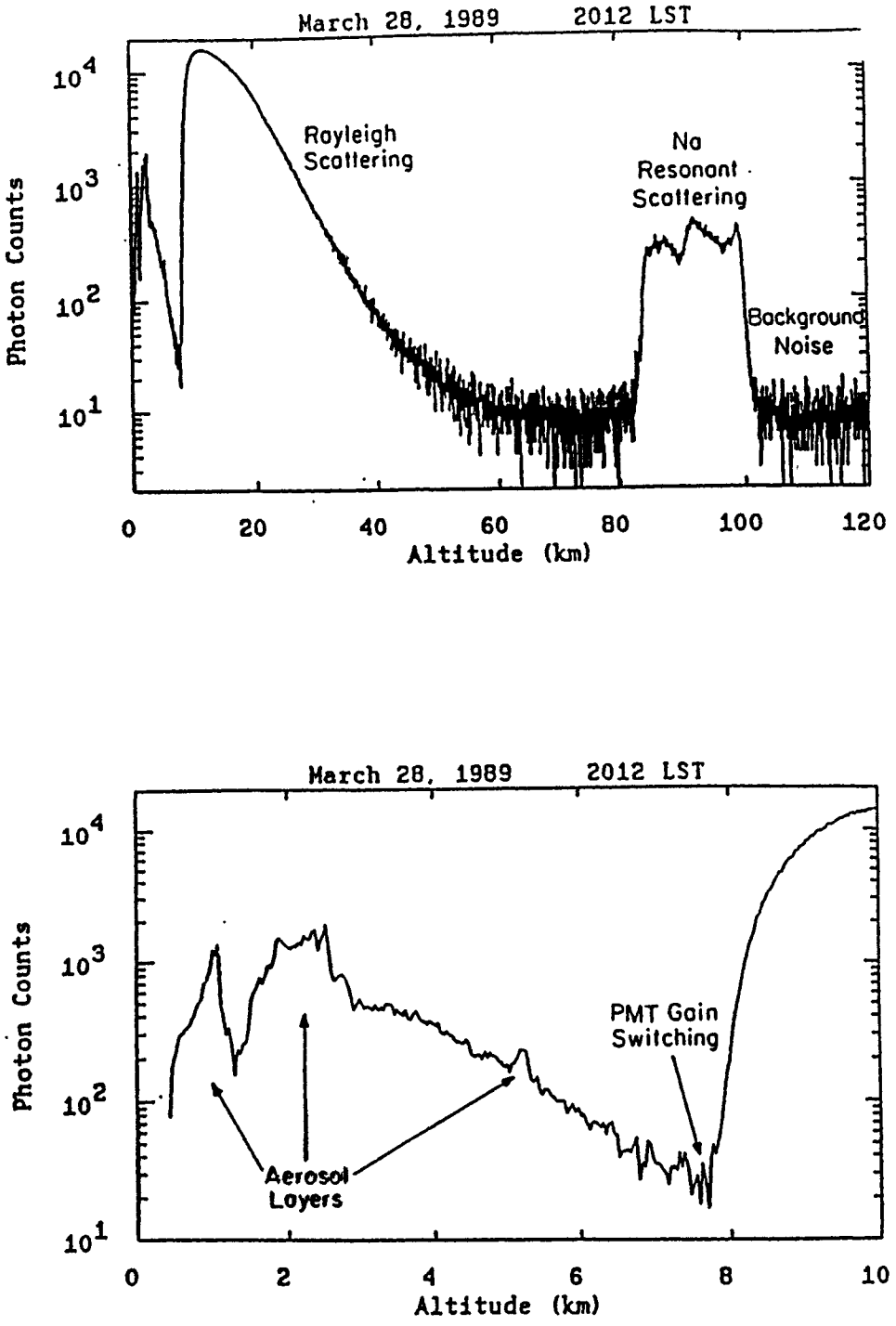

Figure Lidar photon count profile obtained on the night of March 28, 1989 at Arecibo Observatory, Puerto Rico with the UIUC CEDAR Na lidar. The profile was collected by integrating the backscattered signal from 4800 laser shots during a period of 25s starting at 2012 LST. The vertical resolution of the data is 37.5 m. a) Complete profile, b) Expanded low-altitude profile.

LIDAR equation and system performance: The Theoretical performance of any LIDAR system is governed by the Lidar equation.

The expected received photon counts is equate to the product of the system efficiency, number of transmitted photons, probability that he transmitted photon is scattered and probability that the scattered photon is received.

It is given by

$$N_s(z) = \left(\eta T_a^{\,2}\right)\left(\frac{P_L\,\Delta t}{hc/\lambda_L}\right)\left(\sigma_{eff}\;\rho_s(z)\,\Delta z\right)\left(\frac{A_R}{4\pi z^2}\right) + N_B\,R_L\,\Delta t$$

where $N_S(z)$ = Expected backscattered photon in the range interval of $z - \Delta$ to $Z + \Delta_2$

$\rho_s(z)$ = density at z

N_B = expected photon count per range bin for pulse due to background and noise

σ_{eff} = effective molecular scattering cross section

Δz = Range in width

A_R = R_x telescope aperture

λ_L = Wavelength of laser

P_L = Laser power

T_a = One way transmittance of the atmosphere

R_L = Laser pulse rate (s^{-1})

Δt = integration time (S)

η =Lidar efficiency

The absolute atmospheric density can be obtained by subtracting the measured background count and then normalizing the result by the photoncount at an altitude where the absolute density is determined either from independent observation or from a model atmosphere.

$$\rho_a(z) = \frac{Z^2 \rho_a(Z_R)}{Z_R^2} \frac{\left[N_R(z) - N^x{}_B R_L \Delta T\right]}{\left[N_R(z_R) - N^x{}_B R_L \Delta T\right]}$$

In the upper atmosphere (Stratosphere) density perturbation caused by gravity waves and tides are typically a few percent or less so that signal levels of the order of $10^5 - 10^6$ counts are required to measure accurately wave induced fluctuations

Rayleigh Lidar can also be used to get the neutral temperature profile as well. The temperature profile is obtained from the relative atmospheric density profiles by using the hydrostatic equation and the ideal gas law

To obtain temperature, the density profile is integrated downwards using the hydrostatic equation, ideal gas law and an assumed upper air temperature. The initial value could as well be taken from a model, because when the equation has been integrated downward by about 1 ½ scale heights, the calculated temperature is relatively insensitive to the initial temperature. The hydrostatic equation

$$dP = -\rho_a g dz$$

Can be combined with the gas law

$$P = -\rho_a RT/M$$

And integrates to yield

$$T(z) = \frac{T(z_1)\,\rho_a(Z_1)}{\rho_a(z)} + \frac{M}{R}\int_z^{z_1} \frac{g(r)\,\rho_a(r)}{\rho_a(z)}\,dr$$

where $T(z)$ = temperature profile

$P(z)$ = pressure profile

$\rho_a(z)$ = density profile

Zi = altitude of upper level temperature estimated in meters

The atmospheric density appears as a ratio. Therefore to determine temperature it is only necessary to measure the relative density.

Because the atmospheric density decreases exponentially with attitude, it is very difficult to extend the Rayleigh Lidar measurements `beyond 80 km'.

Sodium Lidars use the D_2 line for probing and it is a special class of lidars having enormous potential, extending the useful range upto nearly 100 km.